Development of an equilibrium theory solver applied to pressure swing adsorption cycles used in carbon capture processes

Development of an equilibrium theory solver applied to pressure swing adsorption cycles used in carbon capture processes

Gabriel Oreggioni, Daniel Friedrich, Mauro Luberti, Hyungwoong Ahn and Stefano Brandani*

Scottish Carbon Capture and Storage

School of Engineering, The University of Edinburgh

The King's Buildings, Edinburgh EH9 3FB, UK

Abstract

An equilibrium theory simulator (Esim) for the simulation of cyclic adsorption processes is presented. The equations are solved with a Godunov upwind flux scheme that does not require either the evaluation of characteristics or shock equations or the imposition of a numerical entropy condition to track shocks. Esim is able to simulate non-trace and non-isothermal adsorption systems with any adsorption isotherm. Esim has been validated against gPROMS based simulations that use the full set of governing equations (including mass and heat transfer resistances and axial dispersion) carried out under conditions close to the limits where equilibrium theory is valid. Esim enables the establishment of bounds for the optimal performance of an equilibrium driven separation and requires only the measurement of adsorption isotherms.

Keywords: adsorption dynamics, equilibrium theory, hyperbolic systems, Godunov method, carbon capture, pressure swing adsorption.

*Corresponding author: s.brandani@ed.ac.uk

Notation

Nomenclature		
α	Coefficient defined in Eqs 10 and 11.	s^{-1}
b^0	Pre-exponential Arrhenius coefficient for Langmuir isotherm linear constant	bar^{-1}
C	Total fluid phase concentration.	mol/m^3
$\bar{c}$	Vector of fluid phase concentrations.	mol/m^3
c_i	Concentration of component i in the fluid phase.	mol/m^3
c_i^f	Feed concentration for component i.	mol/m^3
c_i^0	Initial concentration in the bed for component i.	mol/m^3
Cp	Molar heat capacity (gas phase)	J/mol K
cp_s	Mass solid heat capacity at constant pressure.	J/kg K
D	Axial diffusion coefficient.	m^2/s
D_c	Column diameter	m
ε	Bed porosity	
f	Conservative flux	
f_i	Conservative flux for component balance equation.	mol/m^2s
$F^n_{j-\frac{1}{2}}$	Numerical flux on the left boundary of the cell.	
$F^n_{j+\frac{1}{2}}$	Numerical flux on the right boundary of the cell.	
h_f	Volumetric enthalpy.	J/m^3
ΔH_i	Enthalpy of adsorption for component i.	J/mol
h_{molar}	Molar enthalpy.	J/mol
h_{refi}	Reference enthalpy for component i.	J/mol
k_{LDF}	Linear Driving Force constant.	m/s
k_{TE}	Thermal axial dispersion.	W/m K
L	Column length.	m
N_C	Number of components.	
P_{feed}	Feed pressure.	bar
P_{vacuum}	Vacuum Pressure.	bar
q_i	Concentration of the adsorbed phase	mol/m^3
qi^*	Concentration of the adsorbed phase calculated using Isotherm function.	mol/m^3
$\widetilde{q_i}$	Average concentration of adsorbed phase.	mol/m^3
q_s	Adsorbent saturation capacity.	mol/m^3
ρ_s	Solid density.	kg/m^3
s	Characteristic speed.	m/s
Δt	Time step size.	s
t_{ads}	Adsorption step time.	s
t_{blow}	Blowdown step time.	s
t_{press}	Pressurisation step time.	s
t_{purge}	Purge step time.	s
T	Temperature.	K
T^f	Feed temperature.	K
T^0	Initial temperature in the bed.	K
U_g	Volumetric internal energy (gas phase).	J/m^3
U_s	Volumetric internal energy (adsorbent).	J/m^3
v	Interstitial velocity.	m/s

v^f	Interstitial velocity at feed conditions.	m/s
W	Generic variable of interest.	
$\breve{W}$	Spatial average value for the variable of interest.	
Δx	Grid size.	m
y_i^f	Component feed mole fraction.	

Introduction

Pressure Swing Adsorption (PSA) cycles are widely used as gas separation unit operations; examples of industrial applications include hydrogen purification and air separation for the production of both nitrogen and oxygen (Ruthven, 1984; Ruthven et al. 1994). In the case of hydrogen purification and oxygen production the separation is based on equilibrium selectivity. The more strongly adsorbed components are held by the solid and a high purity product is obtained. Production of nitrogen is achieved via a kinetic selectivity because oxygen has a slightly smaller critical diameter and diffuses more rapidly in solids that have critically sized micropores (Ruthven et al. 1994). Clearly in this case the separation is operated far from equilibrium conditions, which would either favour nitrogen due to the larger quadrupole moment or would yield a small equilibrium selectivity if van der Waals forces prevail (Ruthven, 1984). CO_2 post-combustion capture from coal fired power plants using PSA can be achieved using adsorbents that show high equilibrium selectivity (see for example Kikkinides et al., 1993; Krishnamurthy et al., 2014; Webley, 2014), but in this case more complex process configurations are needed because carbon dioxide is the more strongly adsorbed component (see for example Ebner and Ritter, 2002; Luberti et al., 2013; Wang et al., 2013). For these systems, the materials are designed to reduce mass transfer resistances, which are primarily in the macropores (Hu et al., 2014).

The design and optimisation of PSA processes is complex because the system is intrinsically dynamic, depends on a large number of parameters and the simulations have to be carried out until the adsorption columns reach cyclic steady state (CSS) (Cheng et al., 1998; Friedrich et al., 2013 and Simo et al., 2008). For equilibrium driven separations any mass transfer resistance or other terms that lead to dispersion of the separation front will reduce the efficiency of the separation. For this reason, simulations which neglect any effects that lead to dispersion of the separation front can establish optimal bounds on the performance of equilibrium driven separations (Ruthven, 1984; Ruthven et al. 1994). To achieve this, these simulations assume instantaneous mass and heat transfer between the gas and solid phase and negligible axial dispersion. Thus equilibrium theory assumes that the adsorbed phase is in equilibrium with the gas phase: the adsorbed phase concentration is calculated directly from the adsorption isotherm and the gas phase concentration. This simplification reduces the number of differential equations since only the mass and the energy balances in the gas phase have to be solved without mass and heat transfer resistances and axial dispersion terms (Ruthven, 1984). Thus equilibrium theory simulations can establish the range of optimal conditions of the full process from a limited number of experimental equilibrium measurements or molecular simulations (see for example Banu et al., 2013).

Traditional PSA cycle solvers (see for example Ruthven et al. 1994; Kumar et al. 1994; Nilchan and Pantelides, 1998; Sun et al.; 1996; Da Silva et al., 1999; Reynolds et al., 2006; Haghpanah et al. 2013) can be used to mimic the limiting ET case by including very fast mass transfer kinetics and reducing axial dispersion. This method does not take full advantage of the ET simplification but requires the solution of the complete, larger set of equations for both gas and solid phases and furthermore being based on the solution of parabolic PDEs may become unstable, ie some dispersion in the shocks is necessary to stabilise the numerical solution.

Equilibrium theory has been employed by several authors to solve adsorption dynamics and the main results are well summarised by Ruthven (1984) and Ruthven et al. (1994). The importance of equilibrium theory in understanding adsorption dynamics starts from the pioneering work of Glueckauf (1949). Subsequent major contributions can be found in the papers published by Helfferich (1967), Rhee et al (1970 and 1971), Klein (1984) and Basmadjian and Coroyannakis (1986) and in the monograph by Rhee et al. (1989). In most of these articles, simplifying assumptions such as trace adsorption separation and linear or Langmuir equilibrium based systems were considered in order to allow the solution of the system of equations using the method of characteristics. The development of a characteristic based ET solver requires a check for the condition of shock formation, a detailed analysis is needed when using different adsorption isotherms (see for example Mazzotti, 2006). The use of equilibrium theory to PSA was developed mainly by Knaebel and Hill (1985), Kayser and Knaebel (1989) and Pigorini and Le Van (1997 and 1998)who published analytical solutions for isothermal trace PSA systems. Ebner and Ritter (2002) modified the analytical solution presented by Kayser and Knaebel (1989) to simulate PSA cycles aimed at the concentration/production of the strongest adsorbing species with linear equilibrium isotherms.

For the solution of the ET models under non-linear conditions, the typical approach is the use of the method of characteristics (Ruthven, 1984). The difficulties in the application of the method of characteristics for the hyperbolic problem lie in the need to derive specific expressions for the analysis of the condition of the formation of shocks. In the case of multi-component and non-isothermal adsorption systems efficient schemes are needed for the numerical solution of the system under study, which do not require this analysis and are applicable to any adsorption isotherm. Several authors such as Guinot (2003), Leveque (Leveque, 2002) and Toro (Toro, 2009) have developed the use of finite volume based approximate Riemann schemes in the solution of hyperbolic equations arising from the modelling of different engineering problems particularly in the field of wave propagation in fluid dynamics. The Godunov scheme (Godunov, 1962) is the simplest of

these approaches since it assumes that the variables of interest are constant along the finite volume (cell) and during each simulation time step thus it is a first order in space and time scheme; higher order schemes have also been developed (see for example Beam-Warming, 1976 and Lax-Friedrich, 1979). However, for higher order methods oscillations are observed when tracking shocks (Leveque, 2002).

In this contribution we focus on the development of a numerical Godunov type scheme for the solution of the pure hyperbolic equation arising from the mass and energy balance in PSA cycles using the equilibrium theory. The novel tool is capable of simulating multi-component, non-isothermal and non-trace adsorptive separation units. This approach has been previously used in the works published by Loureiro and Rodrigues (1991), Lim et al (2001) and Leveque (2002) for dilute single component isothermal systems which show a single transition. In this particular case, the gas velocity remains constant and the application of the Godunov type scheme is straightforward. Bourdarias et al (2006) employed a wave propagation form of the Godunov method to simulate non trace binary ET adsorption systems but the extension to multiple transitions (multicomponent non-isothermal systems) and arbitrary adsorption isotherms is missing. PSA processes include velocity gradients in the adsorption and desorption steps due to bulk adsorption and industrial systems are usually closer to adiabatic than isothermal operation. In this work, we present the development of a new Godunov based numerical tool (Esim) to solve dynamics associated with non-isothermal multicomponent PSA cycles. This tool resolves the issues related to the variable velocity in the gas phase and allows the use of any adsorption isotherm.

2. Mathematical model

The general equations for the mass and energy balances for the gas phase (assuming plug flow and not considering kinetic energy) are presented in Eqs (1), (2) and (3) (Ruthven, 1984; Walton et al., 2005). Eq. (4) gives the mass balance for the solid phase assuming a Linear Driving Force (LDF) mass transfer model.

$$\varepsilon \frac{\partial C}{\partial t} + \varepsilon \frac{\partial (vC)}{\partial z} + \sum_{i=1}^{Nc} (1-\varepsilon) \frac{\partial \tilde{q_i}}{\partial t} = 0 \qquad (1)$$

$$\varepsilon \frac{\partial c_i}{\partial t} + \varepsilon \frac{\partial (vc_i)}{\partial z} + \varepsilon \frac{\partial \left(-D\, C \frac{\partial x_i}{\partial z}\right)}{\partial z} + (1-\varepsilon) \frac{\partial \tilde{q_i}}{\partial t} = 0 \qquad (2)$$

$$\varepsilon \frac{\partial U_g}{\partial t} + \varepsilon \frac{\partial (v h_f)}{\partial z} + \varepsilon \frac{\partial \left(-k_T \frac{\partial T}{\partial z}\right)}{\partial z} + (1-\varepsilon) \frac{\partial U_s}{\partial t} = 0 \quad (3)$$

$$\frac{\partial \widetilde{q_i}}{\partial t} = k_i^p \frac{A_p}{V_p} (q_i{}^* - q_i) \quad (4)$$

These equations can be simplified due to the following assumptions:

a) Negligible axial mass and thermal dispersion (equilibrium theory).
b) No mass or heat transfer resistances (equilibrium theory).
c) The solid density and the heat capacity for the solid phase are independent of temperature and adsorbed concentration (Ruthven, 1984).
d) The gas phase is considered ideal.
e) No pressure drop along the column.

The dispersion terms in Eq. (2) and (3) can be removed by applying assumption a). By using assumption b) the average concentration in the adsorbed phase $\widetilde{q_i}$ can be replaced by the concentration of the adsorbed phase calculated directly from the isotherm $q_i{}^*$. The resulting system of hyperbolic PDEs implemented in Esim is given by:

$$\varepsilon \frac{\partial C}{\partial t} + \varepsilon \frac{\partial (vC)}{\partial z} + (1-\varepsilon) \sum_{i=1}^{Nc} \frac{\partial q_i^*}{\partial t} = 0 \quad (5)$$

$$\varepsilon \frac{\partial c_i}{\partial t} + \varepsilon \frac{\partial (v c_i)}{\partial z} + (1-\varepsilon) \frac{\partial q_i{}^*}{\partial t} = 0 \quad (6)$$

$$\varepsilon \frac{\partial U_g}{\partial t} + \varepsilon \frac{\partial (v h_f)}{\partial z} + (1-\varepsilon) \frac{\partial U_s}{\partial t} = 0 \quad (7)$$

The internal energy of the solid is calculated from

$$U_s = \rho_s cp_s T - \sum_{i=1}^{Nc} (-\Delta H_i)\, q_i{}^* \quad (8)$$

While the enthalpy and the internal energy for the gaseous phase can be written as:

$$h_f = h_{molar}\ C = \left(\sum_{k=1}^{Nc} \left(y_i \int_{T_{ref}}^{T} Cp_i(T) + h_{ref_i} \right) \right) C \quad (9)$$

$$U_g = (h_{molar} - R\,T)\, C \quad (10)$$

For the non-isobaric steps (pressurisation, evacuation and pressure equalisation), it is assumed that the pressure change with time is proportional to the difference between the pressure in the column and the sources/sinks:

$$\frac{\partial P}{\partial t} = \alpha (P - P_{vacuum}) \quad (11)$$

$$\frac{\partial P}{\partial t} = \alpha(P_{feed} - P) \quad (12)$$

The inlet flow is a function of the difference between the pressure in the column and the source/sink during the pressurisation or blowdown step. The interstitial inlet velocity is one of the unknowns to be determined from the global mass balance for the feed (pressurisation) or product (blowdown) side of the adsorption column (schematics for the column can be found in **Figure 1**). The model equations include the adsorption isotherm, which in general terms can be expressed as

$$q_i^* = f(T, \vec{c}) \quad (13)$$

and the ideal gas law

$$P = CRT \quad (14)$$

Since the mass and the energy balances are a hyperbolic system of equations, only one sided boundary conditions are needed and they correspond to the values of the feed concentrations and temperature.

3. Numerical schemes for the simulation of adsorption dynamics under Equilibrium Theory

3.1 Finite Volume method applied to hyperbolic systems

The simplifying assumptions introduced in section 2 lead to a system of hyperbolic equations which need to be solved by numerical methods. The set of hyperbolic equations that represent the mass and energy balances in the adsorption column and its associated piecewise initial conditions are an example of a Riemann-Cauchy problem (Leveque, 2002); thus numerical methods such as Finite Volume Riemann solvers of the REA (reconstruct-evolve-average) type can be used for the simulation of the equilibrium theory model of PSA processes. The adsorption column is divided into cells each of which is centred on a node z_j. Along each cell the variable of interest is defined by a polynomial function (reconstruction). In the simplest case, this polynomial is a constant function with the average of the variable of interest along this cell. The Riemann problem is solved by using the values at the boundary of the cells at the current time step ($W_{j-\frac{1}{2}}^n$) (evolution) to obtain the average value along the cell at the next time step ($\breve{W}_j^{n+1}$). Figure 1 illustrates how the REA type algorithms work. In the top part of the figure, the column profile at time t is displayed: a constant function is assumed and consequently $W_{j-\frac{1}{2}}^n$ is equal to $\breve{W}_{j-1}^n$; the wave front evolves (as shown by

the lines overlapping the cell boundaries in the bottom part of the figure) and a new average for the variable of interest can be obtained at $t + dt$ as shown by the dashed lines.

The Riemann solvers can use a wave propagation or a numerical flux approach (Leveque, 2002). A deeper analysis of the application of these two approaches for the problem under study is discussed in sections 3.2 and 3.3.

3.2 Wave propagation approach

In the wave propagation approach, the temporal evolution of the average value of the variable of interest ($\breve{W}_j^{n+1}$) is due to waves that propagate along the column. The wave speed ($s_{j-\frac{1}{2}}^{n}$) is calculated using characteristics (smooth solution) or the Rankine-Hugoniot condition (shocks) plus an entropy condition which is needed to determine when a shock takes place (Leveque, 2002).

The equilibrium theory introduces an algebraic constraint which is used to replace $\widetilde{q_i}$ with the equilibrium amount q_i^* in the mass and energy balances (see Eqs. (5) and (6)). Applying the chain rule of differentiation for a generic isotherm in which q_i^* is only a function of the concentration of the species in the gas phase (c_i), the change in adsorbed concentration can be calculated from:

$$\frac{\partial q_i^*}{\partial t} = \sum_{j=1}^{Nc} \frac{\partial {q_i}^*}{\partial c_j} \frac{\partial c_j}{\partial t} = \frac{\partial c_i}{\partial t} \left(\frac{\partial {q_i}^*}{\partial c_i} + \sum_{j \neq i}^{Nc} \frac{\partial {q_i}^*}{\partial c_j} \frac{\partial c_j}{\partial c_i} \right) \tag{15}$$

and the mass balance becomes:

$$\varepsilon \frac{\partial c_i}{\partial t} + \varepsilon \frac{\partial (v c_i)}{\partial z} + (1 - \varepsilon) \frac{\partial c_i}{\partial t} \left(\frac{\partial {q_i}^*}{\partial c_i} + \sum_{j \neq i}^{Nc} \frac{\partial {q_i}^*}{\partial c_j} \right) = 0 \tag{16}$$

which can be rearranged to

$$\frac{\partial c_i}{\partial t} + \frac{1}{\left(1 + \frac{(1-\varepsilon)}{\varepsilon} \left(\frac{\partial {q_i}^*}{\partial c_i} + \sum_{j \neq i}^{Nc} \frac{\partial {q_i}^*}{\partial c_j} \right) \right)} \frac{\partial (v c_i)}{\partial z} = 0 \tag{17}$$

Eq. (17) shows that in the case of using the wave propagation approach, the wave front speed depends strongly on the isotherm. Thus for these solvers, the expression multiplying the spatial derivative has to be evaluated for the values of the concentration on the right and on the left of the cell boundaries in order to check that the characteristics do not increase along the column since this will lead to shock formation. Furthermore, in the case of non-trace systems, the interstitial velocity changes along the column due to sorption effects and thus the global mass balance has to be solved to obtain the evolution of the interstitial velocity v with c_i in the case of smooth solutions.

Bourdarias et al. (2006) used a Riemann wave propagation solver for a binary, non-trace isothermal adsorption systems in which the species obey the Langmuir equilibrium model for an initially empty bed. In this case, a single transition is observed and given the absence of an initial profile, the entropy condition is defined exclusively by the values of the concentration of the feed and the initial condition of the bed; thus for this special case Eq. (17) doesn't need to be evaluated to check whether a shock is taking place. However, for smooth solutions a differential equation has to be solved to determine the change of velocity due to the sorption effects.

For a generic multi-component solver applicable to any isotherm, Eq. (17) as well as the differential equations arising from the global mass balance need to be evaluated in every cell. For isothermal isobaric adsorption systems that obey the Langmuir equilibrium model where there is an initial profile in the column or for non-isothermal or non-isobaric sorption, Eq. (17) must be evaluated to determine the formation of shocks; thus the wave propagation scheme leads to complicated and computationally expensive algebraic-differential equations also for the case of a smooth solution. Nevertheless, these numerical schemes predict accurately the shock formation and the convergence is always guaranteed.

3.3 Numerical flux approach

For hyperbolic equations that can be written in a conservative form (Eq. 18), the temporal evolution of the variable of interest is caused by the gradient of a flux of the same or other variables along the cells thus it is possible to estimate the average value of the variable of interest at the next time step using a defined numerical flux function (see below). The updating expressions for the numerical approach are capable of tracking shock and smooth transitions; neither the imposition of a numerical entropy condition nor the calculation of the characteristics are required thus fewer algebraic or algebraic-differential equations must be solved. However, a careful selection of the simulation step and cell size must be carried out to guarantee stability (imposition of stability conditions).

$$\frac{\partial W(x,t)}{\partial t} + \frac{\partial f(x,t,W)}{\partial x} = 0 \qquad (18)$$

W is the variable of interest, $\widetilde{W_j^n}$ is the spatial average value for W along the cell at one simulation step time and f is the conservative flux which can depend on W. Different expressions for the boundary fluxes $F^n_{j\pm\frac{1}{2}}$as functions of f can be found in the literature, (for example refer to: Godunov, 1962; Lax-Wendroff, 1960; and Beam-Warming, 1976). Godunov (Godunov, 1962) proposed a numerical scheme in which the fluxes at the cell boundaries (Eq. (19)) depend on the average value

of the variable of interest (Eq. (20)) along the previous cell (for positive flow direction). $\widetilde{W}_j^n$ and the numerical flux are assumed to be constant during the simulation step time (Δt) thus the resulting numerical scheme is first order in time and space.

$$F_{j-1/2}^n = \frac{1}{\Delta t}\int_{t_n}^{t_{n+1}} f\left(x_{j-\frac{1}{2}}, t, W\left(x_{j-\frac{1}{2}}, t\right)\right) dt = f\left(x_{j-\frac{1}{2}}, t, \widetilde{W}_{j-1}^n\right) \quad (19)$$

$$\widetilde{W}_j^n = \frac{1}{\Delta x}\int_{x_{j-1/2}}^{x_{j+1/2}} W\,(x,t)\,dx \quad (20)$$

By integrating Eq. (18) and using Eq. (19) and Eq. (20), the following expression for the updating formula can be derived:

$$\widetilde{W}_j^{n+1} = \widetilde{W}_j^n - \frac{\Delta t}{\Delta x}\left(f\left(\widetilde{W}_j^n\right) - f\left(\widetilde{W}_{j-1}^n\right)\right) \quad (21)$$

By applying Eq. (21) to the governing equations of the system, it is possible to convert the coupled PDEs into a system of algebraic nonlinear equations that must be solved in each cell at every simulation step time by using a root finding routine.

3.4 Godunov numerical flux approach solvers applied to adsorption dynamics

The Godunov numerical flux approach must be applied to conservative hyperbolic equations; a conservative variable change (Eqs. (22) - (24)) has been used to transform the component, the global and the energy balances into a suitable form for the application of Godunov's method.

$$W_i = c_i + \left(\frac{1-\varepsilon}{\varepsilon}\right)\widetilde{q_i} \quad (22)$$

$$W_T = C + \left(\frac{1-\varepsilon}{\varepsilon}\sum_{i=1}^{Nc}\widetilde{q_i}\right) \quad (23)$$

$$W_{TE} = \varepsilon U_g + ((1-\varepsilon)U_s) \quad (24)$$

The conservative fluxes can be defined as shown in Eq. (25), Eq. (26) and Eq. (27) respectively.

$$f_i = vc_i \quad (25)$$

$$f_T = vC \quad (26)$$

$$f_{TE} = \varepsilon v h_f \quad (27)$$

One of the assumptions of the Godunov method is that the average value of the variables of interest is constant during the time step thus the numerical fluxes can be written:

$$F^n_{i,j-1/2} = v^n_{j-1}\widetilde{c^n_{i_{j-1}}} \tag{28}$$

$$F^n_{T,j-1/2} = v^n_{j-1}\widetilde{C^n_{j-1}} \tag{29}$$

$$F^n_{TE,j-1/2} = \varepsilon \quad \widetilde{vh_{f_{j-1}}} \tag{30}$$

By applying Godunov's method (Eq. (21)) to the conservative system defined by Eq. (22) to Eq. (30), it is possible to arrive to the updating formula defined by Eq. (31) to Eq. (33)

$$\widetilde{W^{n+1}_{i_j}} = \widetilde{W^n_{i_j}} - \left(\frac{\Delta t}{\Delta x}\left(F^n_{i\ j+1/2} - F^n_{i\ j-1/2}\right)\right) \tag{31}$$

$$\widetilde{W^{n+1}_{T_J}} = \widetilde{W^n_{T_J}} - \left(\frac{\Delta t}{\Delta x}\left(F^n_{T\ j+1/2} - F^n_{T\ j-1/2}\right)\right) \tag{32}$$

$$\widetilde{W^{n+1}_{T_{E\,J}}} = \widetilde{W^n_{T_{E\,J}}} - \left(\frac{\Delta t}{\Delta x}\left(F^n_{T_{E,}\,j+1/2} - F^n_{T_{E,}\,j-1/2}\right)\right) \tag{33}$$

The unknowns in each cell are the concentration of the species at the next time step ($c_{i\,j}^{\,n+1}$) and the velocity (v_j^n) at the current time step. As shown in Fig. 2, the interstitial velocity entering the cell j at time t is known as well as the concentrations of the species. Part of the molecules of the gas are adsorbed thus the interstitial velocity for the gas entering to the next cell is an unknown to be determined as well as the concentration of the species (circled variables) at the time that the front leaves the cell ($t + dt$). The Equilibrium Theory simulator (Esim) obtains the values of these variables by solving the nonlinear system of equations given by Eqs. (22) to (33). Esim has been programmed using the MATLAB software platform and the non-linear equations arising from the discretisation have been solved by employing the FSOLVE (MATLAB, 2015) root finding routine. The FSOLVE function is based on quasi newton method for the solution of algebraic non-linear equations.

4. Breakthrough curve simulations

The results generated by Esim have been validated by comparing them with simulations produced using gPROMS in which the full governing equations for the gas phase and the LDF model for the solid phase have been implemented (Nilchan and Pantelides, 1998). The axial dimension has been discretised using an orthogonal collocation finite element scheme, which is suitable for reversing flows, with a 3rd order polynomial in each element, i.e. a discretisation with 10 elements has 31 nodes. The assumptions of the equilibrium theory are approximated in the gPROMS code by using very small axial dispersion coefficients (1000 times smaller than those estimated from correlations, see Ruthven, 1984) and large mass transfer k_{LDF} values (approx. 10 times larger than the corresponding macropore diffusion control values, see Hu et al., 2014). Higher values lead to numerical instabilities given that a shock is the true solution in an adsorption step with a favourable type I isotherm (Ruthven, 1984).

It must be emphasised that this comparison is intended to validate the correct implementation of the novel tool, given the lack of analytical expressions for the solution of the system under study. The results of the isothermal (Fig. 3) and non-isothermal (Figs 4 to 6) breakthrough simulations show clearly the propagating fronts. For the non-isothermal case, two transitions (Fig. 4) can be observed**:** the first one corresponds to a thermal and concentration shock (Figs 5 and 6) at approx. 77 seconds for which the CO_2 mole fraction reaches an intermediate plateau. At about 1000 seconds, a smooth transition takes place because during the front breakthrough there is still cool gas entering to the column thus a reduction of temperature occurs enabling more CO_2–molecules to be adsorbed. Consequently, after the second transition, the bed is saturated at feed conditions ($y^f_{CO_2}$=0.15, $C^f_{CO_2}$=9.08 mol/m^{3,} , T=298K). For both the isothermal and non-isothermal case Esim manages to track the shocks properly since the breakthrough curves for the sharp transitions present the same first order moment. It can be observed that Esim manages to capture the shock with less smoothing for an equal number of spatial domain discretisation units (150 cells in finite volume method and 51 elements in OCFEM order 3)

The simulation parameters are shown in Table 1, the column dimensions as well as the feed flow correspond to a lab scale PSA rig, the feed compositions replicate the exhaust gas of a coal fired boiler and the adsorbent properties have been taken from Kikkinides et al. (1993). The Langmuir isotherms have been recalculated imposing that the saturation capacity is kept constant for all components respecting thermodynamic consistency (Rao and Sircar, 1999 and Ruthven, 1984).

$$b_i = b_i^0 e^{-\left(\frac{\Delta H_i}{RT}\right)} \quad (34)$$

$$q_i = \frac{q_s b_i P y_i}{1+\sum_{j=1}^{Nc} b_j P y_j} \quad (35)$$

Given that the numerical scheme is trying to capture a pure shock, the resulting smooth profile is a result of the numerical dispersion. The numerical dispersion of the isothermal breakthrough simulations has been quantified by calculating the second moment from the breakthrough curve (Ruthven, 1984):

$$\sigma^2 = 2\int_0^\infty \left(1 - \frac{c_i(t)}{c_{feed}}\right) t dt - \mu^2 \quad (36)$$

where μ is the first order moment given by

$$\mu = \int_0^\infty \left(1 - \frac{c_i(t)}{c_{feed}}\right) dt \quad (37)$$

These equations are strictly valid when the concentration of the adsorbing species is very low (trace isothermal system and the fluid velocity is constant) thus breakthrough curve simulations in which the CO_2 mole fraction is 0.01 with the balance being an inert gas were used. The isothermal breakthrough curves for a trace adsorption system have been simulated using 100, 150, 200 and 400 cells in Esim (Fig. 7). The values for the second order moments for each curve are plotted in Fig. 8 showing that the dispersion is inversely proportional to the square of the number of cells.

5. Cycle simulation and convergence to steady state

Esim has been extended to the solution of PSA cycle dynamics. The cyclic steady state results for a non-isothermal non-trace PSA cycle generated by Esim have been compared with the simulations for the same cycle configuration using gPROMS to validate the correct implementation of all the steps in a cycle. The cycle evolution for pressure, CO_2 mole fraction and temperature at the feed end of the column at CSS are presented in Figs 9.a, b and c respectively, showing very good agreement of the results produced by the two codes. Since Esim simulates a pure equilibrium theory based system cyclic steady state is achieved with a lower number of cycles as seen in Figs 10 a and b. For the gPROMS simulations, a realistic axial dispersion and thermal conductivity coefficients (Wen, 1975) are used thus smoothing the concentration and temperature fronts and reducing numerical instabilities. The comparison confirms that Esim provides reliable predictions for full PSA cycles and that a Godunov type scheme has been implemented for the first time to this complex dynamic system.

Conclusions

In this work, a new Equilibrium Theory PSA cycle solver (Esim) has been introduced. Esim allows the estimation of the equilibrium limiting performance for a given adsorption process and the identification of a set of high separation efficiency configurations by just using the isotherm equilibrium function as input data. The simplifications associated with the Equilibrium Theory and the fact of considering axial dispersion to be negligible convert the mass and the energy balances in an adsorption column into a system of hyperbolic equations. A conservative variable change is defined enabling the use of the Godunov numerical flux. This removes the need of imposing a numerical entropy condition or of calculating the characteristics in each cell.

Esim results have been validated by comparison against simulations using gPROMS in which simulations were undertaken by using micropore equilibrium and macropore LDF model. The assumption of the Equilibrium Theory has been emulated by employing very large values for the k_{LDF} constant and very small values for the axial dispersion coefficients. It can also be observed that Esim manages to properly track shocks and smooth transitions since the first order moment for the breakthrough curves generated by Esim are equal to the ones corresponding to the curves produced by the gPROMS based solver; showing the correct implementation of the novel tool.

The convergence to CSS for the new solver has been demonstrated by simulating a non-isothermal non trace binary adsorption equilibrium based system under conditions of interest in CO_2 post combustion capture technology. Cyclic pressure, CO_2 mole fraction and temperature evolution have been compared against the ones produced by the gPROMS based code and confirm the correct implementation of the new solver to the simulation of full PSA cycles. This comparison also shows that the ET solver requires fewer cycles to reach CSS in comparison with full governing equations thus it indicates that ET simulator can in principle be used for the efficient determination of the limiting Pareto fronts for the optimization of equilibrium based PSA separations.

It can be concluded that the new solver introduced in this work reduces the complexity of the modelling of adsorption dynamics by requiring less empirical data and a simpler code in order to undertake a quick scan of operating conditions and cycle configurations for the design of PSA cycles. Its implementation enables the simulation of generic adsorption systems with any adsorption isotherm without modifying the main code of the solver. The new tool also is a proof of concept of the application of numerical flux method for the solution of complex adsorption dynamics with

rapidly varying flows, presenting a novel approach for the modelling of this kind of separation process.

References

Banu AM, Friedrich D, Brandani S and Duren T. A Multiscale Study of MOFs as Adsorbents in H_2 PSA Purification. Ind. Eng. Chem. Res. 2013; 52: 9946-9957.

Beam RW and Warming RF. Upwind second order difference schemes with applications in aerodynamic flows. AIAA J. 1976; 24: 1241-1249.

Bourdarias C, Gisclon M, Junca S. Some mathematical results on a system of transport equations with an algebraic constraint describing fixed-bed adsorption of gases. J. Math. Anal. Appl. 2006; 313: 551-571.

Cheng YS, Alpay E, Kershenbaum LS. Simulation and optimisation of a rapid pressure swing reactor. Comput. Chem. Eng. 1998; 22: 545-552.

Da Silva F, Silva J, Rodrigues A. A General Package for the Simulation of Cyclic Adsorption Process. Adsorption. 1999; 5: 229-244.

Ebner A, Ritter J. An equilibrium theory analysis of a rectifying PSA for heavy component. AIChE J. 2002; 48: 1679-1691.

Friedrich D, Ferrari MC, Brandani S. Efficient simulation and acceleration of convergence for a dual piston pressure swing adsorption system. Ind. Eng. Chem. Res. 2013; 52: 8897-8905.

Glueckauf E. Theory of chromatography VII. The general theory of two solutes following non-linear isotherm. Discussion of the Faraday Society. 1949; 7: 12-25.

Godunov SK. The problem of a generalized solution in the theory of quasilinear equations in gas dynamics. Russ. Math. Surv. 1962; 17: 145-165.

Guinot V. Godunov Type Schemes: An Introduction for Engineers. Amsterdam: Elsevier. 2003

Haghpanah R, Nilam R, Rajendran A, Farooq S, Karimi IA. Cycle synthesis and optimization of a VSA process for postcombustion CO_2 capture. AIChE J. 2013; 59: 4735-4748.

Helffreich F. Multicomponent ion exchange in fixed beds. Generalized equilibrium theory for systems with constant separation factors. Ind. Eng. Chem. Fundamen. 1967; 6: 362-364.

Hu, X, Mangano, E, Friedrich, D, Ahn, H, Brandani, S. Diffusion mechanism of CO_2 in 13X zeolite beads. Adsorption. 2014; 20: 121–135.

Kayser JC, Knaebel KS. Pressure swing adsorption: Development of an equilibrium theory for binary gas mixtures with non- linear isotherm. Chem. Eng. Sci. 1989; 44: 1-8.

Kikkinides ES, Yang RT, Cho S H. Concentration and recovery of CO_2 from flue gas by pressure swing adsorption. Ind. Eng. Chem. Res. 1993; 32: 2714-2720.

Klein G. Calculation of ideal or empirically modified mass-action equilibria in heterovalent, multicomponent ion exchange Comput. Chem. Eng. 1984; 8: 171-178.

Knaebel KS, Hill FB. Pressure swing adsorption: development of an equilibrium theory for gas separations. Chem. Eng. Sci. 1985; 40: 2351-2360.

Krishnamurthy S, Rao VR, Guntuka S, Haghpanah R, Rajendran A, Amanullah M ,Karimi IA, Farooq S. CO_2 capture from dry flue gas by vacuum swing adsorption: A pilot plant study. AIChE J. 2014; 60: 1830-1842.

Lax PD and Wendroff B. Systems of conservation laws. Commun. Pure Appl Math. 1960; 13: 217–237.

LeVan MD, Costa A, Rodrigues A, Bossy A, Tondeur D. Fixed-bed adsorption of gases: Effect of velocity variations on transition types. AIChE J. 1988; 34: 996-1005.

Leveque R. Finite Volume Methods for Hyperbolic Problems. Cambridge University Press: Cambridge; 2002.

Lim Y I, Le Lann J M, Joulia X. Accuracy, temporal performance and stability comparisons of discretization methods for the numerical solution of Partial Differential Equations (PDEs) in the presence of steep moving fronts. Comput. Chem. Eng. 2001; 25: 1483-1492.

Loureiro J M, Rodrigues A. Two solution methods for hyperbolic systems of partial differential equations in Chemical Engineering. Chem. Eng. Sci. 1991;46:3259-3267.

Luberti M, Friedrich D, Brandani S, Ahn H. Design of H_2 PSA for cogeneration of ultrapure hydrogen and power at an advanced integrated gasification combined cycle with pre-combustion capture. Adsorption. 2013; 20: 511-524.

Mazzotti M. Local equilibrium theory for the binary chromatography of species subject to a generalized Langmuir isotherm. Ind. Eng. Chem. Res 2006; 45: 5332-5350.

MATLAB R2015a, The MathWorks, Inc., Natick, Massachusetts, United States.

Pigorini G, Le Van M D. Equilibrium Theory for Pressure Swing Adsorption.2. Purification and Enrichment in Layered Beds. Ind. Eng. Chem. Res. 1997a; 36:2296-2305.

Pigorini G, Le Van M D. Equilibrium Theory for Pressure Swing Adsorption. 3. Separation and Purification in Two- Component Adsorption. Ind. Eng. Chem. Res. 1997b;36: 2306-2319.

Rao MB and Sircar S. Thermodynamic consistency for binary gas adsorption equilibria. Langmuir 1999; 15: 7258-7267

Reid R, Prausnitz JM, Poling BE. The Properties of Gases and Liquids. McGraw-Hill, New York ;1987.

Reynolds SP, Ebner AD, Ritter JA. Stripping PSA cycles for CO_2 recovery from flue gas at high temperature using a hydrotalcite-like adsorbent. Ind. Eng. Chem. Res. 2006; 45: 4278-4294.

Rhee H K, Aris R, Amudson N. Theory of Multicomponent Chromatography. Philos. Trans. A. Math. Phys. Eng. 1970; 267: 419-455.

Rhee H K, Aris R, Amudson N. Multicomponent adsorption in continuous countercurrent exchangers. Philos. Trans. A. Math. Phys. Eng. 1971; 269: 187-215.

Rhee H K, Aris R, Amudson N. First-Order Partial Differential Equations Vol 2: Theory and Application of Hyperbolic Systems of Quasilinear Equations. Englewood Cliffs: Prentice-Hall; 1989.

Ruthven DM. Principles of Adsorption and Adsorption Processes. New York: Wiley; 1984.

Ruthven DM, Farooq S, Knaebel KS. Pressure Swing Adsorption. New York: VCH, 1994.

Simo M, Brown CJ, Hlavaceck V. Simulation of pressure swing adsorption in fuel ethanol production processes. Comput. Chem. Eng. 2008; 32: 1635-1649.

Sun LM, LeQuere P, Levan MD. Numerical simulation of diffusion-limited PSA process models by finite difference methods. Chem. Eng. Sci. 1996; 51: 5341-5352.

Toro EF. Riemann Solvers and Numerical Methods for Fluid Dynamics: A Practical Introduction. Dordrecht: Springer. 2009

Wang L, Yang Y, Shen W, Kong , Li P, Yu J, Rodrigues A. CO_2 capture from Flue Gas in an Existing Coal-Fired Power Plant by Two Sucessive Pilot-Scale VPSA Units. Ind. Eng. Chem. Res. 2013; 52:7947-7955.

Walton KS, LeVan MD. Effect of energy balance approximations on simulations of fixed-bed adsorption. Ind. Eng. Chem. Res. 2005; 44: 7474-7488.

Webley PA. Adsorption technology for CO_2 separation and capture: a perspective. Adsorption. 2014; 20: 225-231.

Wen CY, Fan LT. Models for Flow Systems and Chemical Reactors. New York: Marcel-Dekker; 1975

LIST OF FIGURES

Table 1: Parameters used for the simulation of the breakthrough curve

Variable	Value	Variable	Value
L (m)	0.5	q_s (mol/m^3)	2233
D_c(m)	0.025	$b^o_{CO_2}$(bar^{-1})	8.41e–6
ε	0.4	$b^o_{N_2}$(bar^{-1})	2.79e–4
Feed Flow (mol/s)	0.0051	$-\Delta H_{CO_2}$ (J/mol)	30558
$y^f_{CO_2}$	0.15	$-\Delta H_{N_2}$(J/mol)	15907
$y^f_{N_2}$	0.85	Cpa_{CO_2}(J/mol K)*	24.47
T^f(K)	298	Cpb_{CO_2}(J/mol K^2)	0.024
ρ_s(kg/m^3)	708	Cpa_{N_2}(J/mol K)	29.41
cp_s(J/kg k)	1046	Cpb_{N_2}(J/mol K^2)	–0.00249
$t_{ads} = t_{purge}$	100	$t_{press} = t_{blow}$	100

*The gas phase heat capacities from Reid et al. (1987) are approximated with a linear relationship (R = 0.99) in the temperature range of interest: $Cp_i(T) = Cpa_i + Cpb_iT$

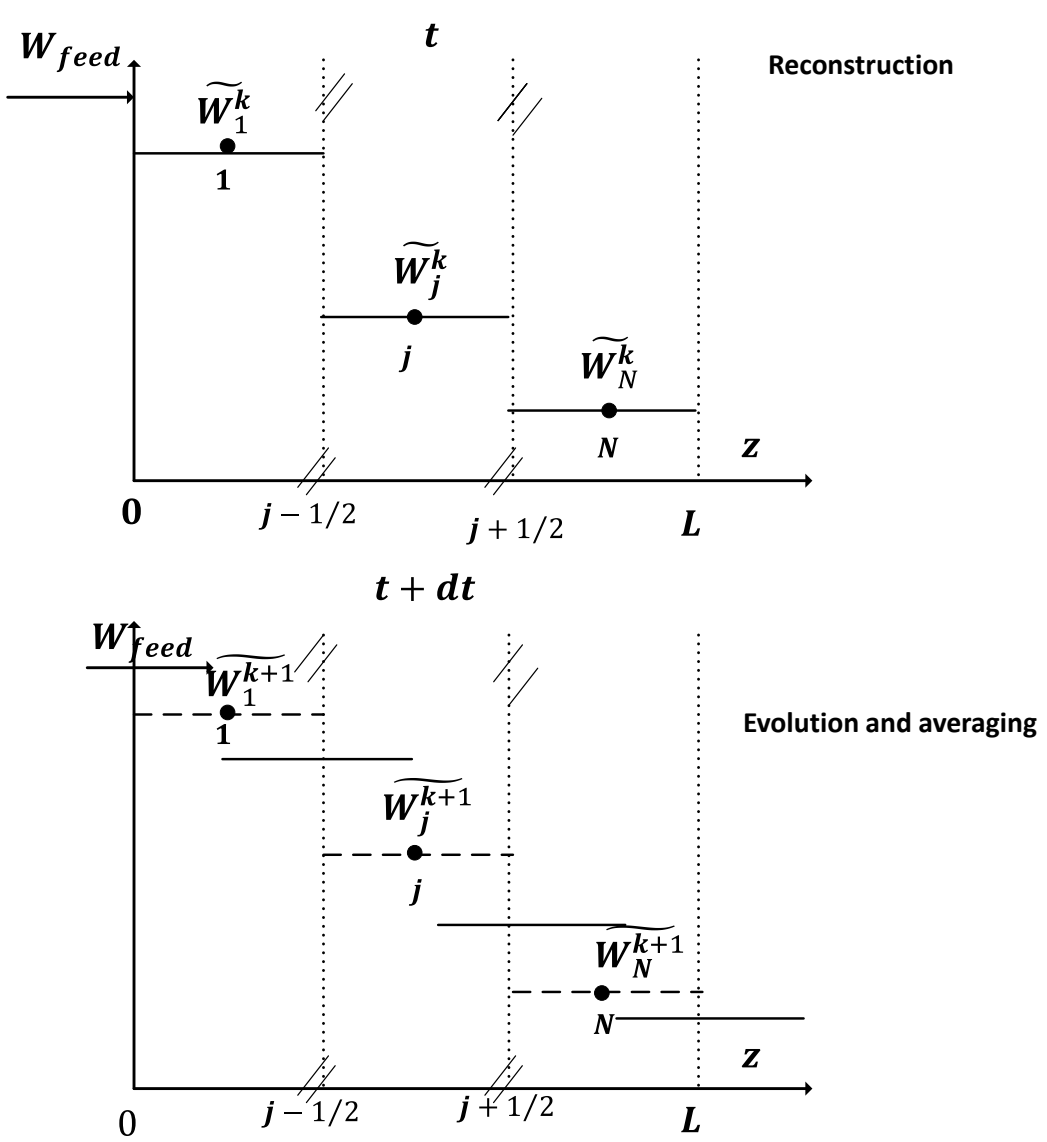
W_{feed}
t
Reconstruction
$\widetilde{W}_1^k$
1
$\widetilde{W}_j^k$
j
$\widetilde{W}_N^k$
N
z
0
$j-1/2$
$j+1/2$
L
$t+dt$
W_{feed}
$\widetilde{W}_1^{k+1}$
1
Evolution and averaging
$\widetilde{W}_j^{k+1}$
j
$\widetilde{W}_N^{k+1}$
N
z
0
$j-1/2$
$j+1/2$
L

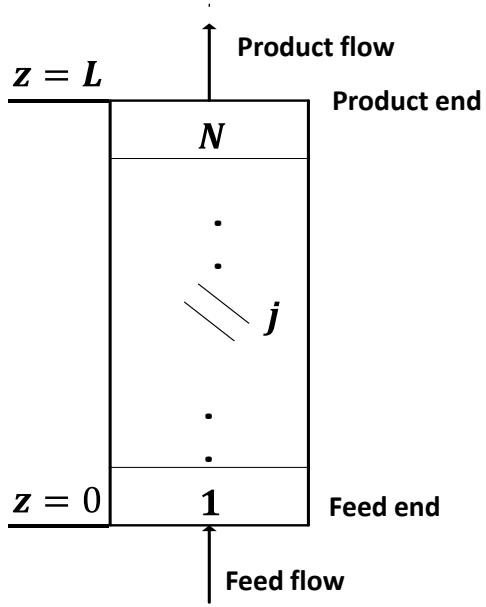
Product flow
$z=L$
Product end
N
j
$z=0$
1
Feed end
Feed flow

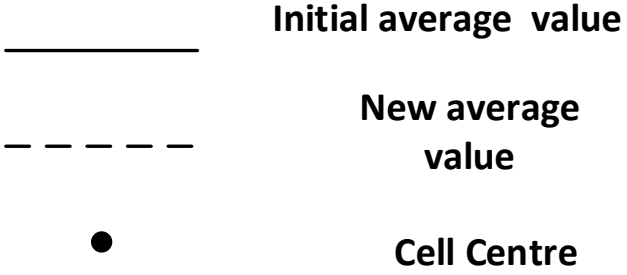
Initial average value
New average value
Cell Centre

Figure 1

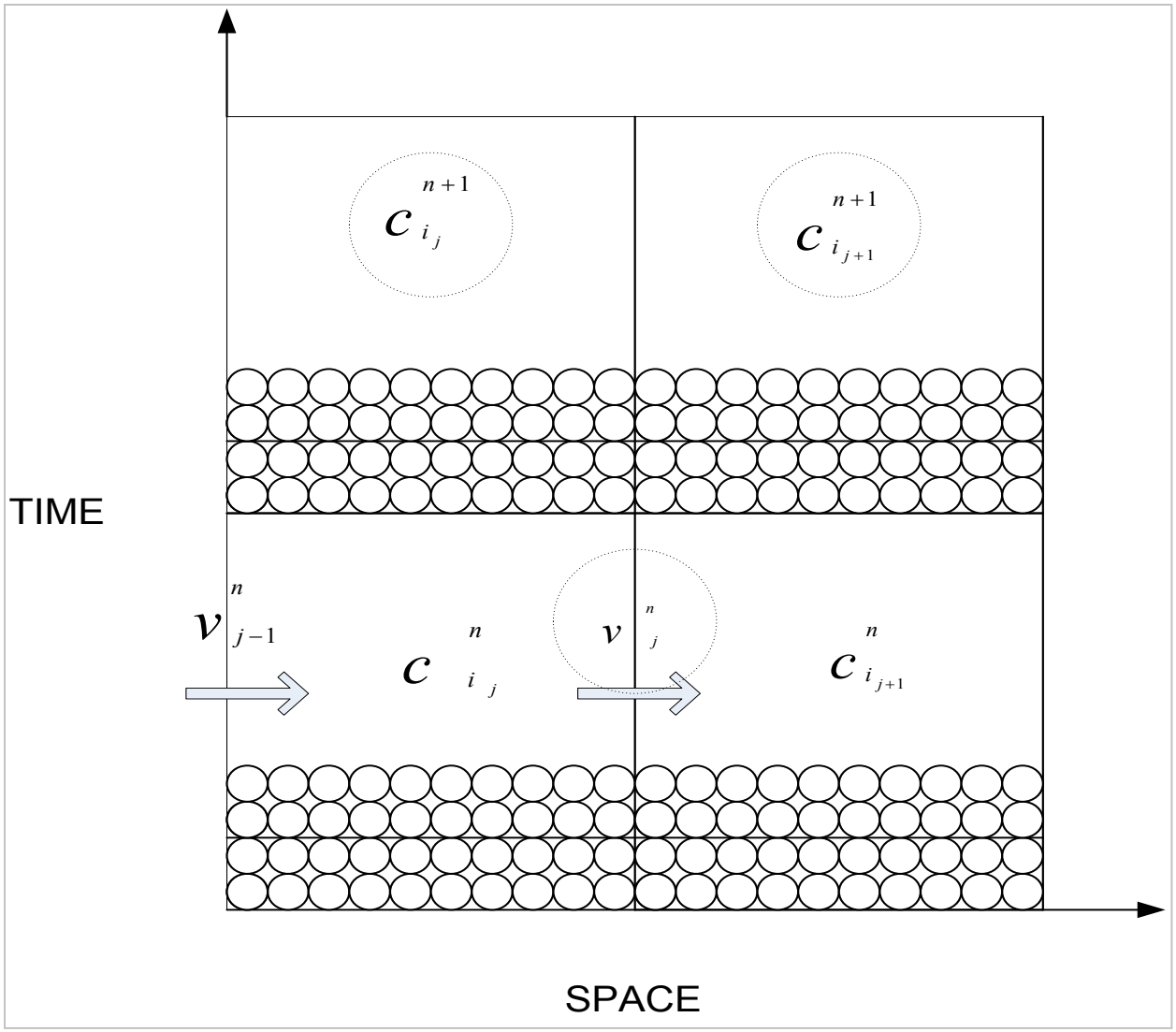

Figure 2

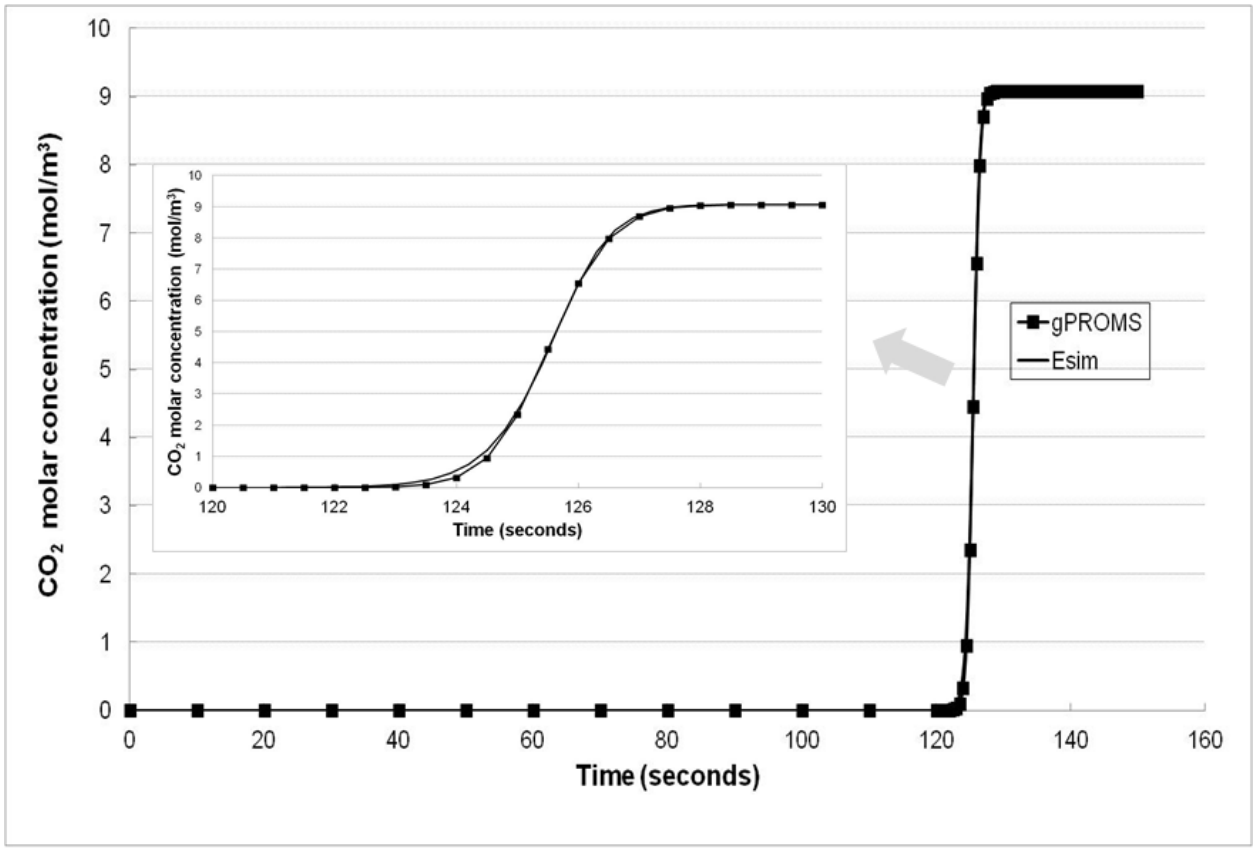
CO_2 molar concentration (mol/m³)
Time (seconds)
gPROMS
Esim
CO_2 molar concentration (mol/m³)
Time (seconds)

Figure 3

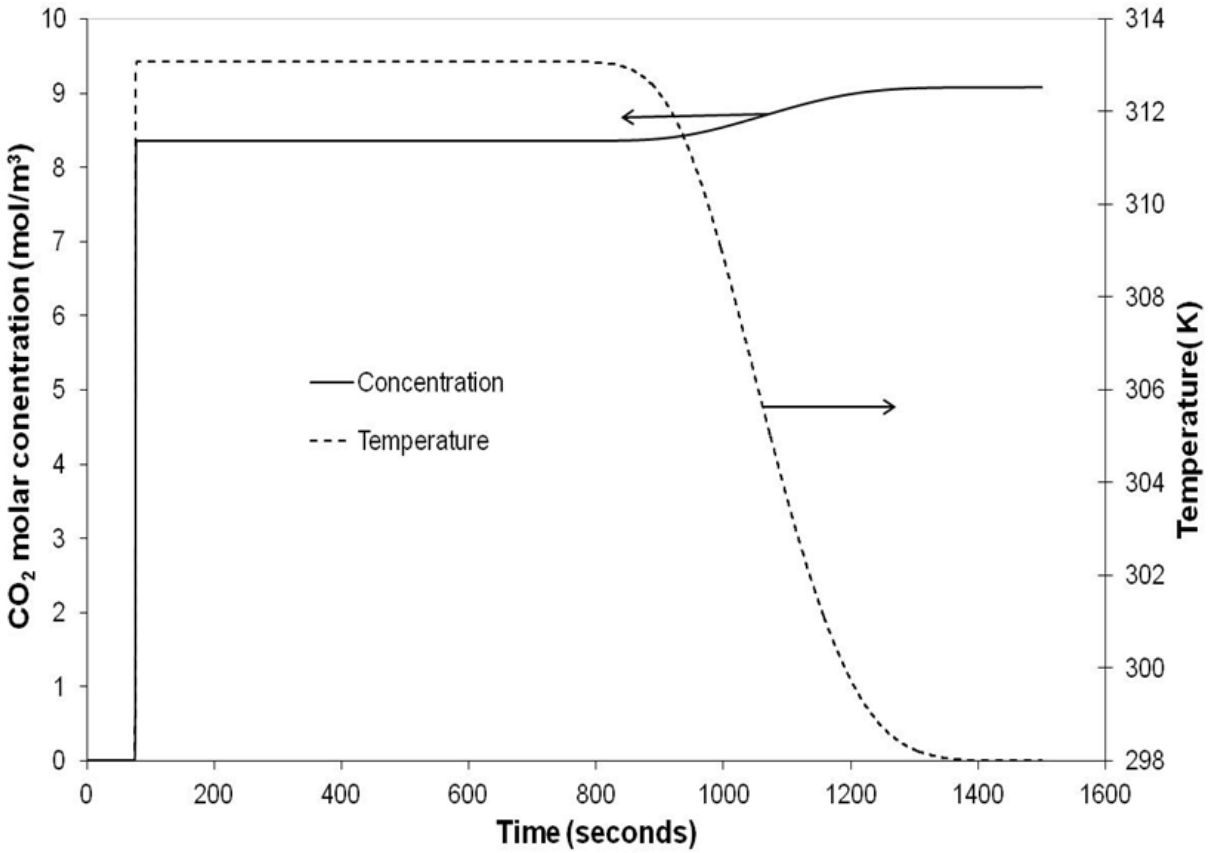
CO_2 molar conentration (mol/m³)
Temperature(K)
Time (seconds)
Concentration
Temperature
0
1
2
3
4
5
6
7
8
9
10
298
300
302
304
306
308
310
312
314
0
200
400
600
800
1000
1200
1400
1600

Figure 4

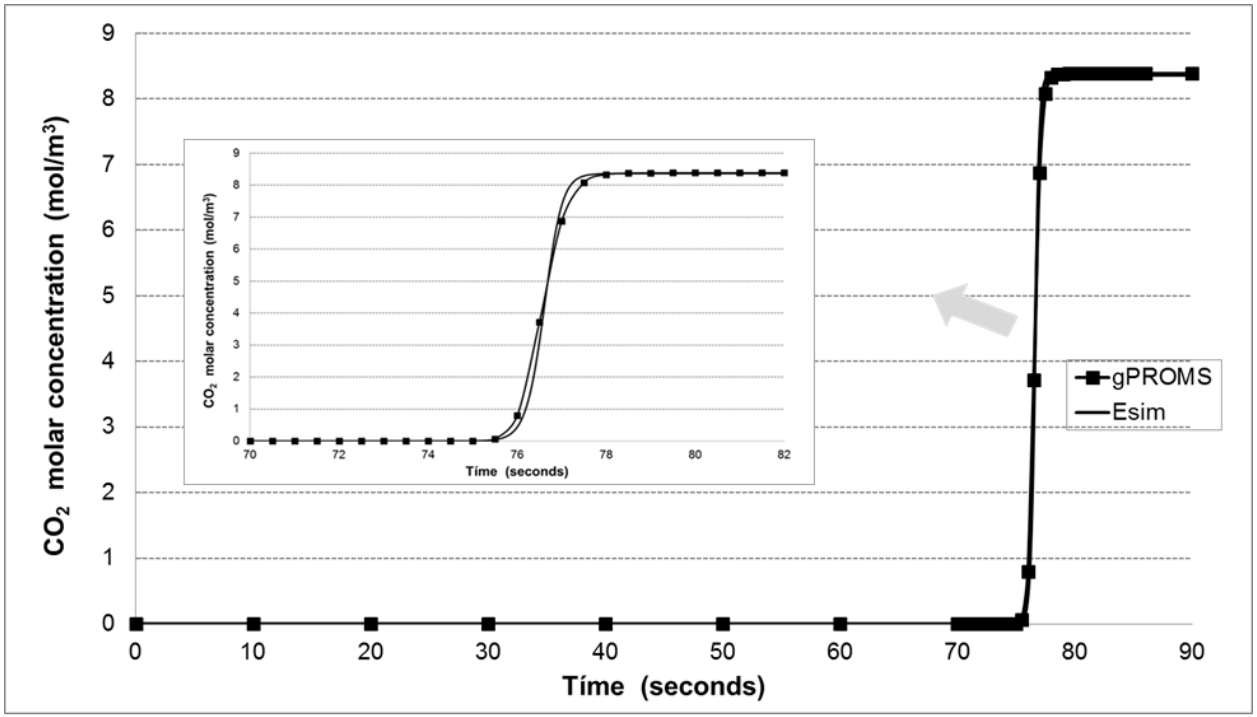
CO_2 molar concentration (mol/m^3)
Time (seconds)
gPROMS
Esim
CO_2 molar concentration (mol/m^3)
Time (seconds)

Figure 5

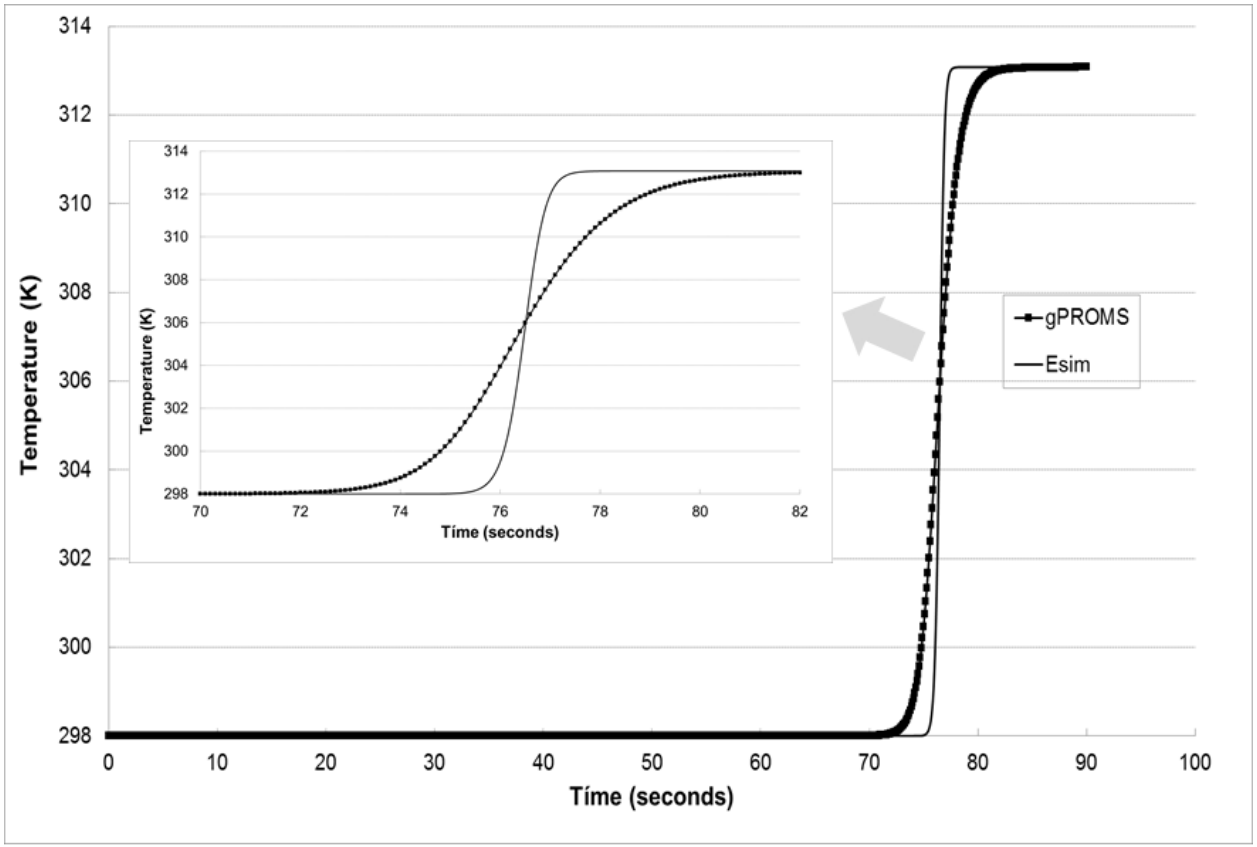
Temperature (K)
Time (seconds)
gPROMS
Esim
314
312
310
308
306
304
302
300
298
0
10
20
30
40
50
60
70
80
90
100
70
72
74
76
78
80
82

Figure 6

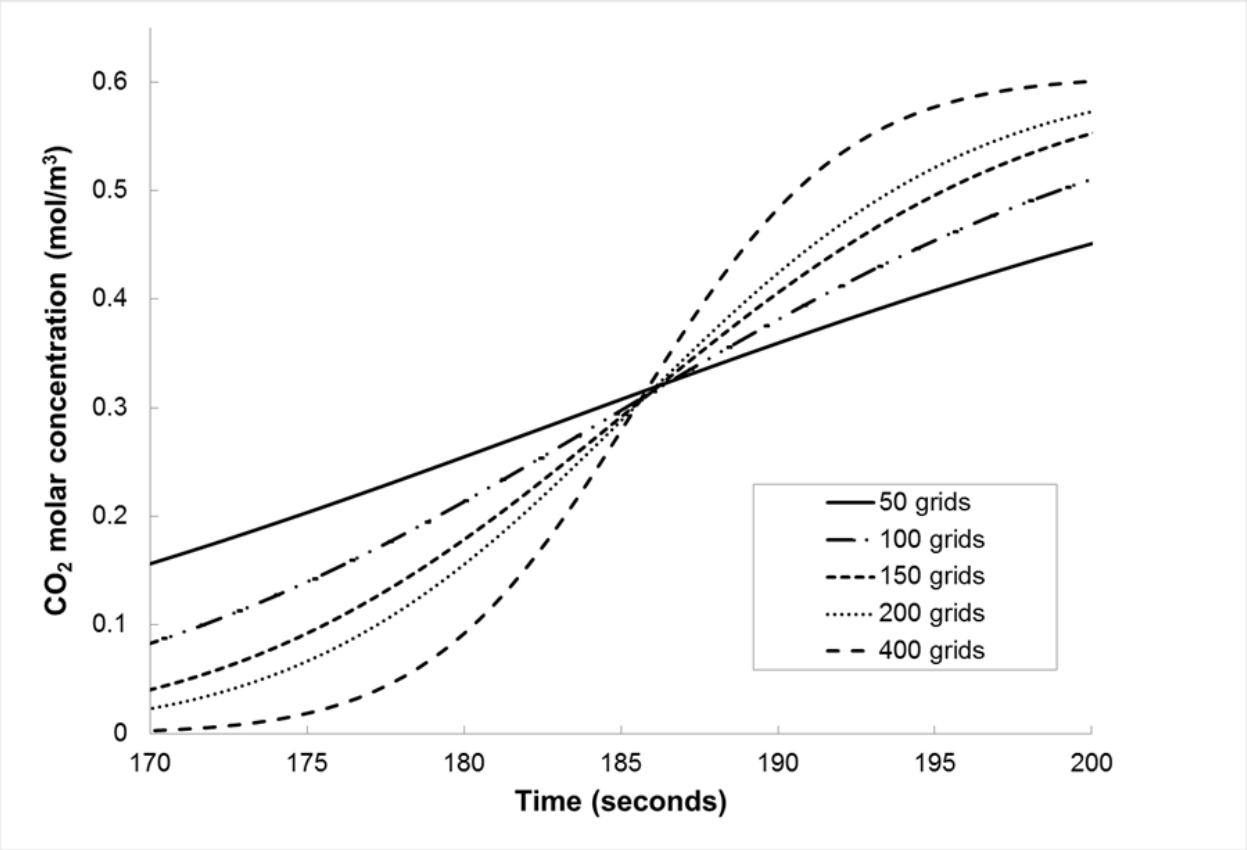
0.6
0.5
0.4
0.3
0.2
0.1
0
CO_2 molar concentration (mol/m^3)
170
175
180
185
190
195
200
Time (seconds)
50 grids
100 grids
150 grids
200 grids
400 grids

Figure 7

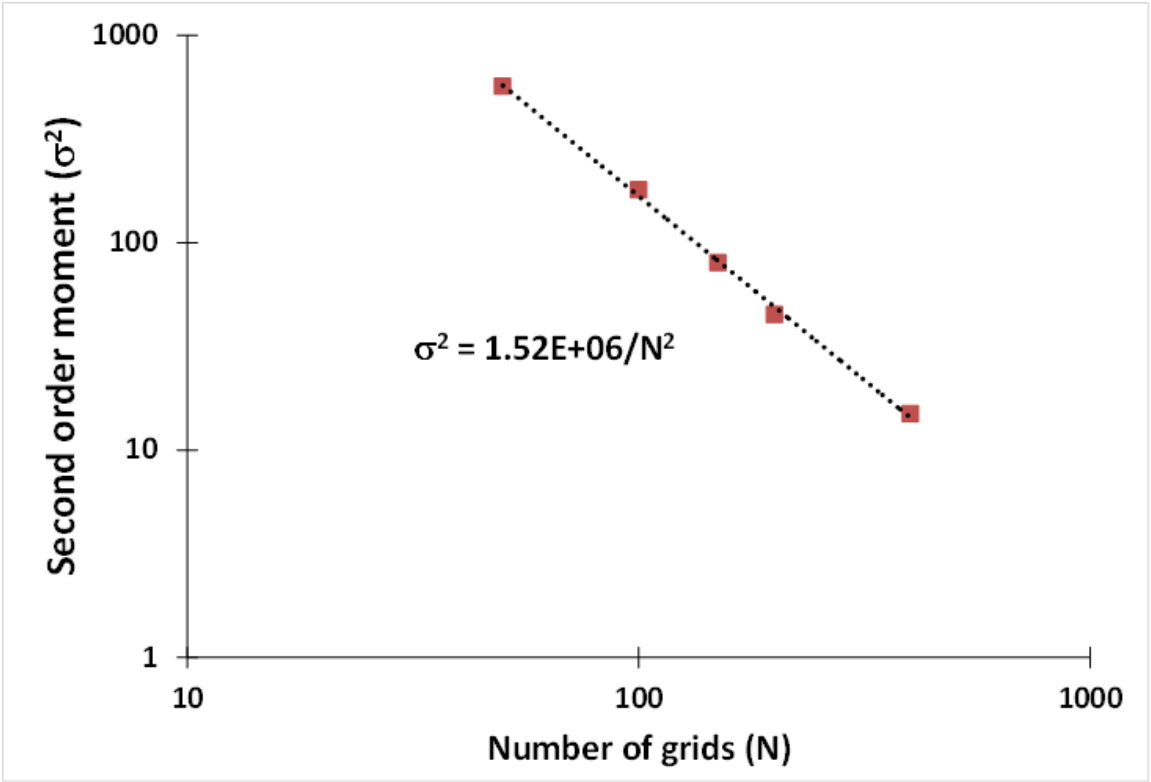
1000
100
10
1
Second order moment (σ^2)
σ^2 = 1.52E+06/N^2
10
100
1000
Number of grids (N)

Figure 8

a

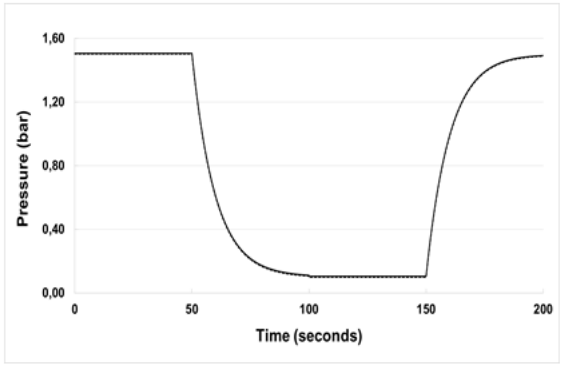
Pressure (bar)
1,60
1,20
0,80
0,40
0,00
0
50
100
150
200
Time (seconds)

b

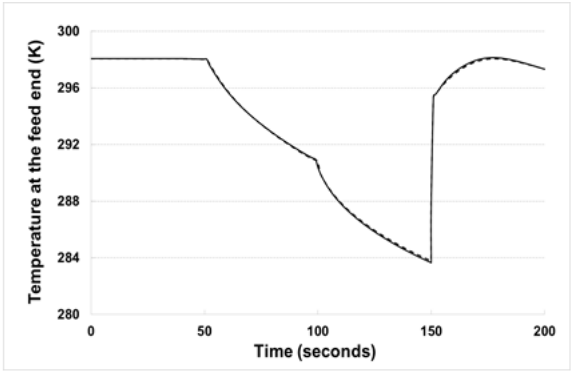
Temperature at the feed end (K)
300
296
292
288
284
280
0
50
100
150
200
Time (seconds)

c

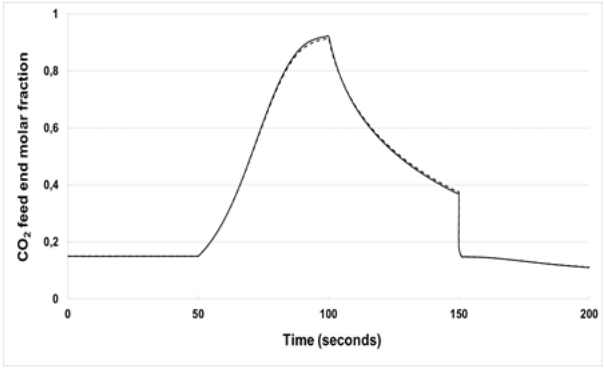
CO_2 feed end molar fraction
1
0,8
0,6
0,4
0,2
0
0
50
100
150
200
Time (seconds)


gPROMS
Esim

Figure 9

a

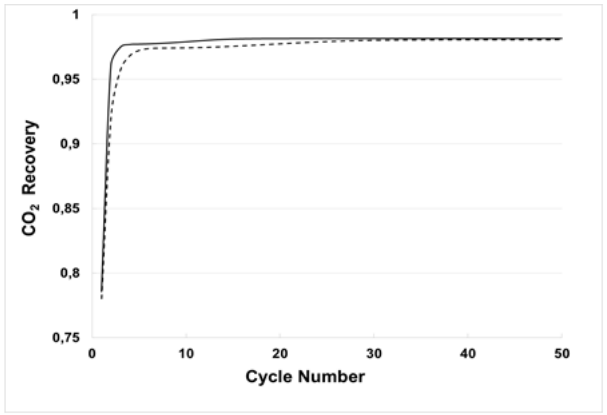
1
0,95
0,9
0,85
0,8
0,75
CO_2 Recovery
0
10
20
30
40
50
Cycle Number


Recovery_gPROMS
Recovery_Esim

b

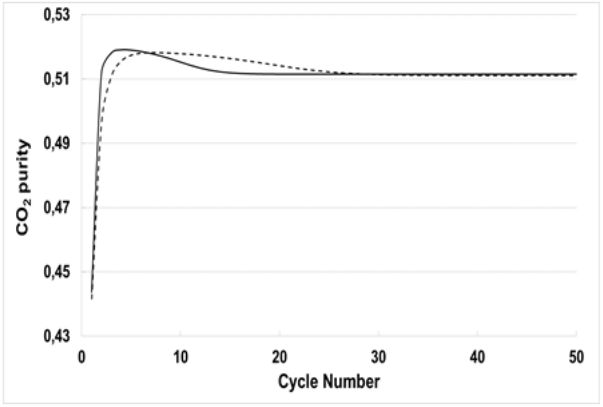
0,53
0,51
0,49
0,47
0,45
0,43
CO_2 purity
0
10
20
30
40
50
Cycle Number

Figure 10